International Forum on Aeroelasticity and Structural Dynamics
IFASD-2019-001
June 10-13, Savannah, GA, USA

FLUTTER PREDICTION BASED ON DYNAMIC EIGEN DECOMPOSITION OF COUPLED CFD-CSD FLIGHT SIMULATION

Kim[1], T.,

[1]Pegase Avtech
Bothell, WA, USA
johnkim@pegaseavtech.com

Thomas[2], J.P., Dowell[3], E.H.

[2,3]Department of Mechanical Engineering and Materials Science
Duke University
Durham, NC, USA
jthomas@duke.edu, earl.dowell@duke.edu

Keywords: Flutter prediction, dynamic eigen decomposition, dynamic eigenmodes, frequency-domain stability, CFD-CSD simulation, gust response

Abstract: During the design and analysis of aircraft flutter boundaries are typically computed using the p-k iterations, k iterations, p iterations, or eigenvalue analysis, that require computationally expensive and numerically sensitive procedures especially for complex configurations. In this work, the Dynamic Eigen Decomposition (DED) and a frequency domain stability theorem developed previously will be applied to a coupled CFD-CSD simulation to predict the aircraft flutter. It is known that the dynamic eigenmodes (DE) of the aeroelastic system are an intrinsic property of the system independent of dynamic pressure and flutter mode is identical to one of the DEs. Thus, the aeroelastic instability can be predicted by simply extrapolating the corresponding dynamic eigenvalues obtained at low, subcritical dynamic pressures. We will extend the theory to show that this is also true in the case of two parameters where air speed as well as air density vary. The proposed scheme is applied to computationally simulated flight data of F-16 wing model with a bending and a torsion mode shape subjected to a vertical gust in a transonic flow. It is shown that the new approach produces very accurate flutter predictions with the gust response. It is also shown that the single parameter variation of dynamic pressure based on a mean, constant speed of sound can yield sufficiently accurate flutter results.

1. INTRODUCTION

In this work, aircraft flutter will be predicted using the DED technique developed recently [1-5]. In the previous work [4,5] it was shown that when the perturbed aeroelastic equation of motion at a given dynamic pressure is decomposed into the DEs, the critical flutter point can be predicted

by a simple extrapolation of the corresponding dynamic eigenvalues in the frequency domain. Furthermore, the flutter mode is identified as one of the DEs implying that the flutter solution is invariant under the change of dynamic pressure. Thus, the method provides a powerful tool to predict the flutter based on data obtained at subcritical dynamic pressures, i.e., at dynamic pressures lower than the flutter dynamic pressure. In particular, since it captures the vital fluid-structure interaction mechanism correctly using only the structural part of the aeroelastic response it can be used effectively for flight flutter testing and simulation. For further demonstration of the flutter prediction scheme, we simulate a flight flutter testing scenario using computational aeroelasticity that couples CFD (Computational Fluid Dynamics) and CSD (Computational Structural Dynamics) in a transonic flow regime. For the airplane model we use the F-16 wing with one bending and one torsion modes, and for the CFD we use a Reynolds Averaged Navier-Stokes solver. The excitation input to the wing is a uniform vertical gust. Frequency responses of the modal displacements due to the gust are extracted at two altitudes and the flutter stability is checked by extrapolating the dynamic eigenvalues using the Nyquist diagram in frequency domain. Alternatively, the (2×2) full aeroelastic equation of motion is also processed to yield the flutter solution with a higher accuracy. It is shown that in both types of simulations, the predicted flutter solution is very close to the known exact solution, within 4.4% and .6%, respectively, satisfying the following requirements desirable for computational simulation or flight flutter testing:

1. The flutter prediction is conducted entirely using the simulation or test data alone without relying on solving any analytical models.
2. The procedure is executed at low dynamic pressures, sufficiently lower than the flutter point to provide for the safety of test pilot and airplane.
3. Only structural data, i.e., displacements and velocities on the lifting surface, are used with no aerodynamic measurements required.

2. DYNAMIC EIGEN DECOMPOSITION OF AEROELASTIC SYSTEM

A structural dynamic system described by *N* structural modes is given in discrete-time, state-space as

$$\boldsymbol{z}^{n+1} = \boldsymbol{A}_s \boldsymbol{z}^n + \boldsymbol{B}_s \boldsymbol{y}^n + \boldsymbol{B}_i \boldsymbol{u}^n \quad (2N \times 1) \tag{1}$$

Similarly, an unsteady aerodynamic system in *M* states undergoing statically nonlinear, dynamically linear (SNLDL) oscillations can be described by [4]

$$\begin{aligned} \boldsymbol{x}^{n+1} &= \boldsymbol{A}_a \boldsymbol{x}^n + \boldsymbol{B}_a \boldsymbol{z}^n \quad (M \times 1) \\ \boldsymbol{y}^n &= q_D \, (\boldsymbol{C}_a \boldsymbol{x}^n + \boldsymbol{D}_a \boldsymbol{z}^n) \, (2N \times 1) \end{aligned} \tag{2}$$

One can write the coupled fluid structural interaction (FSI) equation subject to *varying dynamic pressure, q_D but at a constant Mach number* as follows:

$$\boldsymbol{X}^{n+1} = \boldsymbol{A}(q_D)\boldsymbol{X}^n + \boldsymbol{B}\boldsymbol{u}^n \ \ (L \times 1) \tag{3}$$

$$(L = 2 \times N + M)$$

where

$$\boldsymbol{X} \equiv \begin{Bmatrix} \boldsymbol{x} \\ \boldsymbol{z} \end{Bmatrix}$$
$$\boldsymbol{A}(q_D) \equiv \begin{bmatrix} \boldsymbol{A}_a & \boldsymbol{B}_a \\ q_D\boldsymbol{B}_s\boldsymbol{C}_a & \boldsymbol{A}_s + q_D\boldsymbol{B}_s\boldsymbol{D}_a \end{bmatrix}, \boldsymbol{B} \equiv \begin{bmatrix} 0 \\ \boldsymbol{B}_i \end{bmatrix} \tag{4}$$

Splitting $\boldsymbol{X}$ into *nominal* and *perturbed* parts:

$$\boldsymbol{X} = \boldsymbol{X}_0 + \Delta\boldsymbol{X} \tag{5}$$

where $\boldsymbol{X}_0$ and $\Delta\boldsymbol{X}$ each satisfies,

$$\boldsymbol{X}_0^{n+1} = \boldsymbol{A}(q_{D0})\boldsymbol{X}_0^n + \boldsymbol{B}\boldsymbol{u}^n \ : \text{Nominal}$$
$$\boldsymbol{\Delta X}^{n+1} = \boldsymbol{A}(q_D)\boldsymbol{\Delta X}^n + \boldsymbol{\Delta A}\boldsymbol{X}_0^n \ : \text{Perturbed} \tag{6}$$

where $\boldsymbol{\Delta A} \equiv \Delta q_D \overline{\boldsymbol{\Delta A}}$, $\Delta q_D \equiv q_D - q_{D0}$ and

$$\overline{\boldsymbol{\Delta A}} \equiv \begin{bmatrix} \boldsymbol{0} & \boldsymbol{0} \\ \boldsymbol{B_s C_a} & \boldsymbol{B_s D_a} \end{bmatrix} = Const \tag{7}$$

In the above derivation, the key assumptions are:

1. The nominal aeroelastic system is *stable*.
2. Along the Constant Mach Varying Altitude (CMVA) air speed is assumed constant and only density changes.
3. The perturbed system is stable or unstable only depending on Δq.

Note that 2. is a good approximation of the so-called matched point state of atmosphere. More specifically, considering that the speed of sound and hence the true air speed varies with respect to altitude only within $\pm 7.5\%$ from its mean value (Fig. 1) and also that only one of the two terms in the downwash boundary condition is affected by the change in air speed, it is reasonable to ignore the variation and use the mean value. Hence, we will regard dynamic pressure as the single varying parameter. See Ref. 4 for a detailed discussion. Based on these assumptions, flutter is

determined by the dynamic instability of the perturbed system which has the following transfer function of the perturbed equation from $\boldsymbol{X_0^n}$ to $\boldsymbol{\Delta X^{n+1}}$:

$$\boldsymbol{G}(\omega) = [z\boldsymbol{I} - \boldsymbol{A}(q_D)]^{-1}\boldsymbol{\Delta A} \equiv \boldsymbol{V}_v(\omega)\boldsymbol{\Lambda}_v(\omega)\boldsymbol{W}_v^{\dagger}(\omega) \tag{8}$$

where $z \equiv e^{j\omega\Delta t}$ and

$$v \equiv rank\big(\boldsymbol{G}(\omega)\big) = rank(\overline{\boldsymbol{\Delta A}}) = 2N$$

$\boldsymbol{\Lambda_v} =$ $(v \times v)$ diagonal matrix with nonzero dynamic eigenvalues

$\boldsymbol{V_v}, \boldsymbol{W_v} =$ matrices of right and left dynamic eigenvectors

$\boldsymbol{V}_v(\omega)\boldsymbol{W}_v^{\dagger}(\omega) = \boldsymbol{I}_v$ *(orthonormality)*

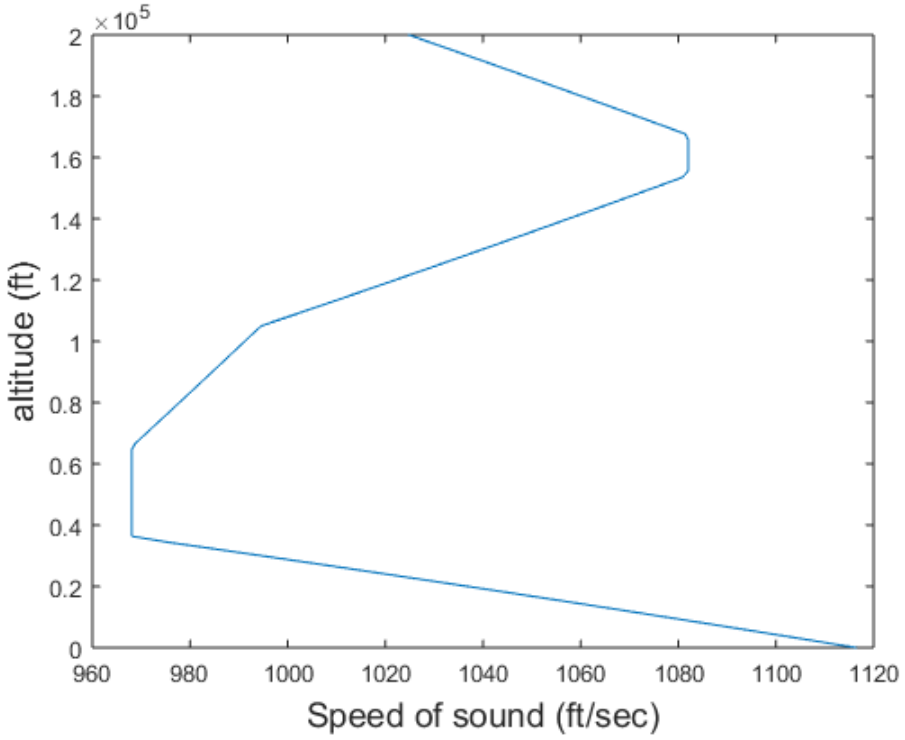

Fig. 1 Altitude vs. speed of sound of standard atmosphere

It can be shown that the following transfer function is '*modally equivalent'* to $\boldsymbol{G}(\omega)$ [1].

$$\boldsymbol{G}'(\omega) = [z\boldsymbol{I} - \boldsymbol{A}(q_{D0})]^{-1}\boldsymbol{\Delta A} \equiv \boldsymbol{V}'_v(\omega)\boldsymbol{\Lambda}'_v(\omega)\boldsymbol{W}_v^{\dagger\prime}(\omega) \tag{9}$$

That is,

$$\boldsymbol{V}'_{\nu}(\omega) \equiv \boldsymbol{V}_{\nu}(\omega), \boldsymbol{W}'_{\nu}(\omega) \equiv \boldsymbol{W}_{\nu}(\omega)$$
$$\boldsymbol{\Lambda}'_{\nu}(\omega) \equiv [\boldsymbol{I}_{\nu} + \boldsymbol{\Lambda}_{\nu}(\omega)]^{-1}\boldsymbol{\Lambda}_{\nu}(\omega) \tag{10}$$

and the two systems share the same set of dynamic eigenmodes, $\boldsymbol{V}_{\nu}(\omega)$ and $\boldsymbol{W}_{\nu}(\omega)$.

3. STABILITY OF AEROELASTIC SYSTEMS BASED ON DYNAMIC EIGENVALUES

Suppose the dynamic pressure is increased by $\kappa \Delta q_D$ instead of Δq_D from the nominal q_{D0}. Then $\boldsymbol{G}(\omega)$ will be modally equivalent to

$$\boldsymbol{G}'(\omega) = [z\boldsymbol{I} - \boldsymbol{A}(q_{D0})]^{-1}k\boldsymbol{\Delta A} \equiv \boldsymbol{V}_{\nu}(\omega)\kappa\boldsymbol{\Lambda}'_{\nu}(\omega)\boldsymbol{W}^{T}_{\nu}(\omega) \tag{11}$$

which has new eigenvalues $\kappa\lambda'_{\nu i}(\omega)$ but retains the same dynamic eigenvectors. Hence, the dynamic eigenvalues of the new perturbed syst. can be expressed as

$$\boldsymbol{\Lambda}_{\nu}(\omega) \equiv [\boldsymbol{I}_{\nu} - \kappa\boldsymbol{\Lambda}'_{\nu}(\omega)]^{-1}\kappa\boldsymbol{\Lambda}'_{\nu}(\omega) \tag{12}$$

Since $\boldsymbol{v}_{\nu i}(t)$'s, $\boldsymbol{w}_{\nu i}(t)$'s are invariant under $\kappa \Delta q_D$ and bounded by the orthonormality, the stability of the transfer function and therefore the flutter boundary should be determined by $\lambda_{\nu i}(t)'$s $(i = 1,2, \ldots 2N)$. Thus, invoking the Multi-Input Multi-Output (MIMO) Nyquist Stability Theorem, one can make the following statement about the stability of the aeroelastic system:

"For a stable aeroelastic equation of motion undergoing a change in dynamic pressure, the Nyquist plot of $det[\boldsymbol{I}_{\nu} - \kappa\boldsymbol{\Lambda}'_{\nu}(\omega)]$ *must not encircle the origin* of the complex plane." (See Fig. 2)

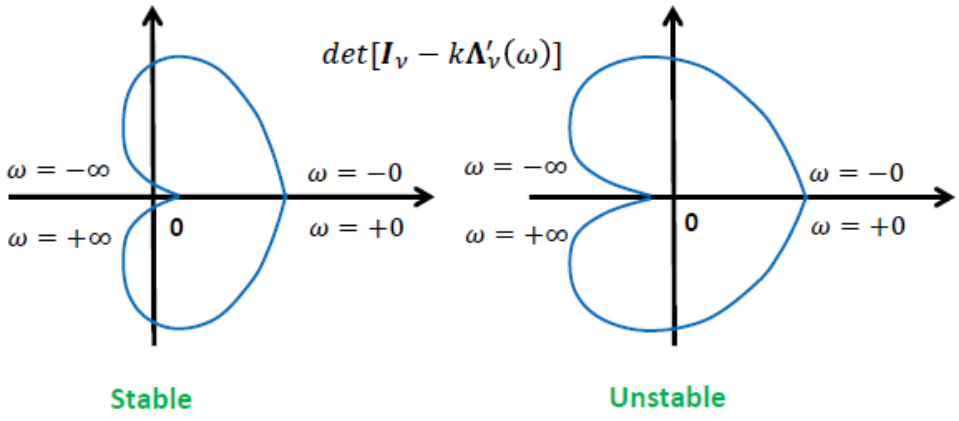

Fig. 2 Stable and unstable MIMO systems according to Nyquist Stability

4. FREQUENCY-DOMAIN FORMULATION WITH STRUCTURAL RESPONSES

Since there are exactly 2N complex or N pairs of complex conjugate dynamic eigenvalues that are not zeros, the stability formulation can be written more conveniently using the structural dynamic equation of motion in the frequency-domain:

$$\boldsymbol{M}\ddot{\boldsymbol{q}} + \boldsymbol{C}\dot{\boldsymbol{q}} + \boldsymbol{K}\boldsymbol{q} = q_D\boldsymbol{Q}(k)\boldsymbol{q} \quad (N \times 1) \tag{13}$$

where k is the reduced frequency ($\equiv \frac{\omega b}{V}$). As before, let $\boldsymbol{q} = \boldsymbol{q}_0 + \Delta\boldsymbol{q}$ such that

$$\begin{aligned} \boldsymbol{M}\ddot{\boldsymbol{q}}_0 + \boldsymbol{C}\dot{\boldsymbol{q}}_0 + \boldsymbol{K}\boldsymbol{q}_0 &= q_{D0}\boldsymbol{Q}(k)\boldsymbol{q}_0 \ : \text{Nominal} \\ \boldsymbol{M}\Delta\ddot{\boldsymbol{q}} + \boldsymbol{C}\Delta\dot{\boldsymbol{q}} + \boldsymbol{K}\Delta\boldsymbol{q} &= q_D\boldsymbol{Q}(k)\Delta\boldsymbol{q} + \Delta q_D\boldsymbol{Q}(k)\boldsymbol{q}_0 \ : \text{Perturbed} \end{aligned} \tag{14}$$

and compute the transfer function from $\boldsymbol{q}_0$ to $\boldsymbol{\Delta q}$:

$$\begin{aligned} \boldsymbol{G}_q(\omega) &\equiv [-\omega^2\boldsymbol{M} + j\omega\boldsymbol{C} + \boldsymbol{K} - q_D\boldsymbol{Q}(k)]^{-1}\Delta q_D\boldsymbol{Q}(k) \\ &= [-\omega^2\boldsymbol{M} + j\omega\boldsymbol{C} + \boldsymbol{K} - q_D\boldsymbol{Q}(k)]^{-1}[-\omega^2\boldsymbol{M} + j\omega\boldsymbol{C} + \boldsymbol{K} - q_{D0}\boldsymbol{Q}(k)] - \boldsymbol{I}_N \\ &\equiv \boldsymbol{T}_q(\omega)\boldsymbol{T}_{q0}^{-1}(\omega) - \boldsymbol{I}_N \end{aligned} \tag{15}$$

Note that it requires two transfer functions $\boldsymbol{T}_{q0}$, $\boldsymbol{T}_q$, at the two dynamic pressures, q_{D0} and q_D. Taking DED of $\boldsymbol{G}_q(\omega)$

$$\boldsymbol{G}_q(\omega) \equiv \boldsymbol{V}_N(\omega)\boldsymbol{\Lambda}_N(\omega)\boldsymbol{W}_N^{\dagger}(\omega) \tag{16}$$

leads to the MIMO stability as before. When the dynamic pressure is increased from q_D to $q_D + \kappa\Delta q_D$, the new eigenvalues are obtained as:

$$[\boldsymbol{I}_N - \kappa\boldsymbol{\Lambda}_N(\omega)]^{-1}\kappa\boldsymbol{\Lambda}_N(\omega) \tag{17}$$

The critical dynamic pressure is then obtained as

$$q_{Df} = q_D + \kappa_f\Delta q_D \tag{18}$$

where at least one of $1 - \kappa_f\lambda_{Ni}(\omega_f)$'s vanishes.

5. FREQUENCY-DOMAIN FORMULATION WITH VELOCITY VARIATION

If one were to consider variations in air speed as well as air density with respect to altitude, Eq. (15) would need to be modified to:

$$\begin{aligned}\boldsymbol{G}'_q(\omega) &\equiv \boldsymbol{T}'_{q1}(\omega)\boldsymbol{T}'^{-1}_{q0}(\omega) - \boldsymbol{I}_N \\ &\equiv \left[-\omega^2\boldsymbol{M} + j\omega\boldsymbol{C} + \boldsymbol{K} - \left(q_D\boldsymbol{Q}(k)\right)_1\right]^{-1}\left[-\omega^2\boldsymbol{M} + j\omega\boldsymbol{C} + \boldsymbol{K} - \left(q_D\boldsymbol{Q}(k)\right)_0\right] - \boldsymbol{I}_N \\ &= [-\omega^2\boldsymbol{M} + j\omega\boldsymbol{C} + \boldsymbol{K} - (q_D\boldsymbol{Q}(k))_1]^{-1}\Delta(q_D\boldsymbol{Q}(k)) \end{aligned} \quad (19)$$

where

$$\begin{aligned}\Delta(q_D\boldsymbol{Q}(k)) &\equiv (q_D\boldsymbol{Q}(k))_1 - (q_D\boldsymbol{Q}(k))_0 \\ &= q_{D1}\boldsymbol{Q}(k_1) - q_{D0}\boldsymbol{Q}(k_0) \\ &= \Delta q_D\boldsymbol{Q}(k_1) + q_{D0}[\boldsymbol{Q}(k_1) - \boldsymbol{Q}(k_0)] \end{aligned} \quad (20)$$

and $k_0 \equiv \frac{\omega b}{V_0}, k_1 \equiv \frac{\omega b}{V_1}$, $\Delta q_D \equiv q_{D1} - q_{D0}$. It is assumed that the speed of sound and density change with respect to altitude according to the standard atmospheric state equation say, $f(\rho, V, h) = 0$. For practical purposes, one can approximate the generalized aerodynamic force matrix at the new air speed as,

$$\boldsymbol{Q}(k_1) \approx \boldsymbol{Q}(k_0) + \frac{\partial \boldsymbol{Q}}{\partial k}(k_0)\Delta k = \boldsymbol{Q}(k_0) + \frac{\partial \boldsymbol{Q}}{\partial V}(V_0)\Delta V \quad (21)$$

ignoring the higher order terms because, as discussed above, the effect of the variation in air speed would be small. Hence, inserting (21) into (20) and (19) yields

$$\begin{aligned}&\left[-\omega^2\boldsymbol{M} + j\omega\boldsymbol{C} + \boldsymbol{K} - \left(q_D\boldsymbol{Q}(k)\right)_1\right]^{-1}\left[-\omega^2\boldsymbol{M} + j\omega\boldsymbol{C} + \boldsymbol{K} - \left(q_D\boldsymbol{Q}(k)\right)_0\right] - \boldsymbol{I}_N \\ &\quad \approx [-\omega^2\boldsymbol{M} + j\omega\boldsymbol{C} + \boldsymbol{K} - (q_D\boldsymbol{Q}(k))_1]^{-1}[\Delta q_D\boldsymbol{Q}(k_1) + q_{D0}\frac{\partial \boldsymbol{Q}}{\partial V}(V_0)\Delta V] \end{aligned} \quad (22)$$

Note that Eq. (22) reduces to Eq. (15) if $\Delta V = 0$ or we ignore the speed variation. For instance, in 35,000 ft $<$ h $<$ 65,000 ft (Fig. 1) Eq. (15) will be valid to use.

Now suppose that the aircraft undergoes variations both in air density and air speed by the incremental factors, $\kappa\Delta q_D$, $l\Delta V$, respectively by changing its altitude from h_1 to $h_1 + \Delta h$ following the Constant Mach curve. In reality, air density and speed cannot change independently as they are both functions of the altitude, but for simplicity we will keep both $\kappa\Delta q_D$ and $l\Delta V$ in the equation. Then, the new perturbed aeroelastic response to consider would be,

$$\boldsymbol{\Delta q} \equiv \left[-\omega^2\boldsymbol{M} + j\omega\boldsymbol{C} + \boldsymbol{K} - (q_D\boldsymbol{Q}(k))_1 - \kappa\Delta q_D\boldsymbol{Q}(k_1) - lq_{D0}\frac{\partial \boldsymbol{Q}}{\partial V}(V_0)\Delta V\right]^{-1} \cdot$$
$$[\kappa\Delta q_D\boldsymbol{Q}(k_1) + lq_{D0}\tfrac{\partial \boldsymbol{Q}}{\partial V}(V_0)\Delta V]\boldsymbol{q}_0 \quad (23)$$

subject to the standard atmospheric equation. Invoked by Appendix B of Ref. [6], we will express the perturbed response (23) as a *sum* of two perturbed responses $\boldsymbol{\Delta q}_1$ and $\boldsymbol{\Delta q}_2$ undergoing $\kappa\Delta q_D$ and $l\Delta V$, respectively, as $\boldsymbol{\Delta q} = \boldsymbol{\Delta q}_1 + \boldsymbol{\Delta q}_2$:

$$\boldsymbol{\Delta q}_1 \equiv [-\omega^2\boldsymbol{M} + j\omega\boldsymbol{C} + \boldsymbol{K} - (q_D\boldsymbol{Q}(k))_1 - \kappa\Delta q_D\boldsymbol{Q}(k_1)]^{-1}\kappa\Delta q_D\boldsymbol{Q}(k_1)(\boldsymbol{q}_0 + \boldsymbol{\Delta q}_2) \quad (24)$$
$$\boldsymbol{\Delta q}_2 \equiv \left[-\omega^2\boldsymbol{M} + j\omega\boldsymbol{C} + \boldsymbol{K} - (q_D\boldsymbol{Q}(k))_1 - lq_{D0}\frac{\partial \boldsymbol{Q}}{\partial V}(V_0)\Delta V\right]^{-1} lq_{D0}\frac{\partial \boldsymbol{Q}}{\partial V}(V_0)\Delta V(\boldsymbol{q}_0 + \boldsymbol{\Delta q}_1) \quad (25)$$

If we use DED of the two transfer functions,

$$[-\omega^2\boldsymbol{M} + j\omega\boldsymbol{C} + \boldsymbol{K} - (q_D\boldsymbol{Q}(k))_1]^{-1}\Delta q_D\boldsymbol{Q}(k_1) \equiv \boldsymbol{V}_1(\omega)\boldsymbol{\Lambda}_1(\omega)\,\boldsymbol{W}_1^{\dagger}(\omega) \quad (26)$$
$$[-\omega^2\boldsymbol{M} + j\omega\boldsymbol{C} + \boldsymbol{K} - (q_D\boldsymbol{Q}(k))_1]^{-1}q_{D0}\frac{\partial \boldsymbol{Q}}{\partial V}(V_0)\Delta V \equiv \boldsymbol{V}_2(\omega)\,\boldsymbol{\Lambda}_2(\omega)\boldsymbol{W}_2^{\dagger}(\omega) \quad (27)$$

(24), (25) can be rewritten,

$$\boldsymbol{\Delta q}_1 = \boldsymbol{V}_1(\omega)[\boldsymbol{I} - \kappa\boldsymbol{\Lambda}_1(\omega)]^{-1}\kappa\boldsymbol{\Lambda}_1(\omega)\,\boldsymbol{W}_1^{\dagger}(\omega)(\boldsymbol{q}_0 + \boldsymbol{\Delta q}_2) \quad (28)$$
$$\boldsymbol{\Delta q}_2 = \boldsymbol{V}_2(\omega)[\boldsymbol{I} - l\boldsymbol{\Lambda}_2(\omega)]^{-1}l\boldsymbol{\Lambda}_2(\omega)\,\boldsymbol{W}_2^{\dagger}(\omega)(\boldsymbol{q}_0 + \boldsymbol{\Delta q}_1) \quad (29)$$

Therefore, the perturbed solution is a convolution superposition of $\boldsymbol{V}_1$ and $\boldsymbol{V}_2$:

$$\boldsymbol{\Delta q} = \boldsymbol{V}_1(\omega)\boldsymbol{p}_1(\omega) + \boldsymbol{V}_2(\omega)\boldsymbol{p}_2(\omega) \quad (30)$$

with the two amplitudes determined by

$$\begin{bmatrix} \boldsymbol{I} & -[\boldsymbol{I} - \kappa\boldsymbol{\Lambda}_1]^{-1}\kappa\boldsymbol{\Lambda}_1\,\boldsymbol{W}_1^{\dagger}\boldsymbol{V}_2 \\ -[\boldsymbol{I} - l\boldsymbol{\Lambda}_2]^{-1}l\boldsymbol{\Lambda}_2\,\boldsymbol{W}_2^{\dagger}\boldsymbol{V}_1 & \boldsymbol{I} \end{bmatrix}\begin{Bmatrix}\boldsymbol{p}_1\\ \boldsymbol{p}_2\end{Bmatrix} = \begin{bmatrix}[\boldsymbol{I} - \kappa\boldsymbol{\Lambda}_1]^{-1}\kappa\boldsymbol{\Lambda}_1\,\boldsymbol{W}_1^{\dagger}\\ [\boldsymbol{I} - l\boldsymbol{\Lambda}_2]^{-1}l\boldsymbol{\Lambda}_2\,\boldsymbol{W}_2^{\dagger}\end{bmatrix}\boldsymbol{q}_0 \quad (31)$$

from which one can determine the flutter by checking for what combination of $(\kappa_f, l_f, \omega_f)$ $\boldsymbol{\Delta q}$ diverges. Note that neither $\boldsymbol{I} - \kappa\boldsymbol{\Lambda}_1(\omega)$ nor $\boldsymbol{I} - l\boldsymbol{\Lambda}_2(\omega)$ could be singular because now the aircraft moves through the altitudes satisfying $f(\rho, V, h) = 0$. An important consequence of Eq. (30) and (31) is that the flutter mode will be a linear convolution superposition of $\boldsymbol{V}_1(\omega_f)$ and $\boldsymbol{V}_2(\omega_f)$. In

this regard, the flutter mode can be regarded as *an intrinsic property* of the aeroelastic system as it is in the case of the single parameter variation, Δq.

A word is in order about the efficiency of accounting for the variation in air speed. Unlike the case of the single parameter variation, calculating the DED of Eqs. (26) and (27) requires knowledge of $\boldsymbol{Q}(k_1)$ and $\frac{\partial \boldsymbol{Q}}{\partial V}(V_0)$ which cannot be deduced solely from measuring the aircraft responses. As will be seen in the results, however, the flutter prediction based on the variation in dynamic pressure and hence the manipulation of the single parameter κ alone yields an excellent match with the true flutter solution. Therefore, for all practical purposes and considering the complexity of introducing the second parameter l, the two parameters flutter prediction formulated in this section will be taken as a supplement to the original single parameter formulation and all subsequent calculations will be based on the variation of the κ parameter.

6. FLUTTER PREDICTION WITH A GUST EXCITATION

Ref. [5] discusses how, using the *virtual control inputs (VCI) technique,* the original DED can be modified to cope with cases in which more responses are available than inputs. In practice, only a few control inputs would be available during flight test. Normally, control surfaces – aileron, flap, rudder, elevator – or a gust excitation are used to excite the airplane externally, and this number is much smaller than the number of sensors installed on the aircraft. The new flutter prediction methodology requires an equal number of inputs and outputs and hence the VCI will provide the artificial extra inputs necessary for this requirement. See the Ref. [5] for details.

In this study, we are particularly interested in using frequency responses of the aircraft subject to a gust input. The aeroelastic equation of motion can be written,

$$\boldsymbol{M}\ddot{\boldsymbol{q}} + \boldsymbol{C}\dot{\boldsymbol{q}} + \boldsymbol{K}\boldsymbol{q} - q_D\boldsymbol{Q}(k)\boldsymbol{q} = q_D\boldsymbol{Q}_g(k)\alpha_g \quad (N \times 1) \tag{32}$$

where α_g is the incremental angle of attack caused by the vertical gust and $\boldsymbol{Q}_g(k)$ is the unsteady gust aerodynamics in the modal coordinates. Since the gust represents a single excitation, given N structural coordinates or O sensor outputs we need (N-1) or (O-1) extra excitations and they will be generated by the VCIs.

7. NUMERICAL EXAMPLE OF SIMULATED FFT: F-16 WING IN TRANSONIC FLOW

The proposed scheme is applied to the F-16 wing model with two main structural modes in bending and torsion. The aerodynamic modeling that accounts for compressibility as well as viscosity is done using a Reynolds Averaged Navier-Stokes solver developed at Duke University, while the structural modeling is done with FEM (Finite Element Model). The natural frequencies of the two modes are 8.167878 and 8.671919 *Hz*. The frequency responses of the structural modes are computed by executing the coupled CFD-CSD solver. Fig. 3 shows the computational grids generated to model the unsteady transonic flow around the wing. For theoretical and computational backgrounds of the algorithms and computer codes, see Ref. [7-11]. The gust input is simplified

to be uniformly distributed over the wing. Thus, any time delay effects between different sections of the wing are ignored. This is a good approximation for the wing with a short chord relative to the characteristic gust length. As stated above, we will use the vertical gust as our mean to excite the wing. Hence, to have the (2×2) transfer function matrix it is necessary to add one extra column of the frequency responses by the VCI method mentioned above. Only the single parameter flutter prediction based on Eq. (15) is performed to calculate the onset of flutter.

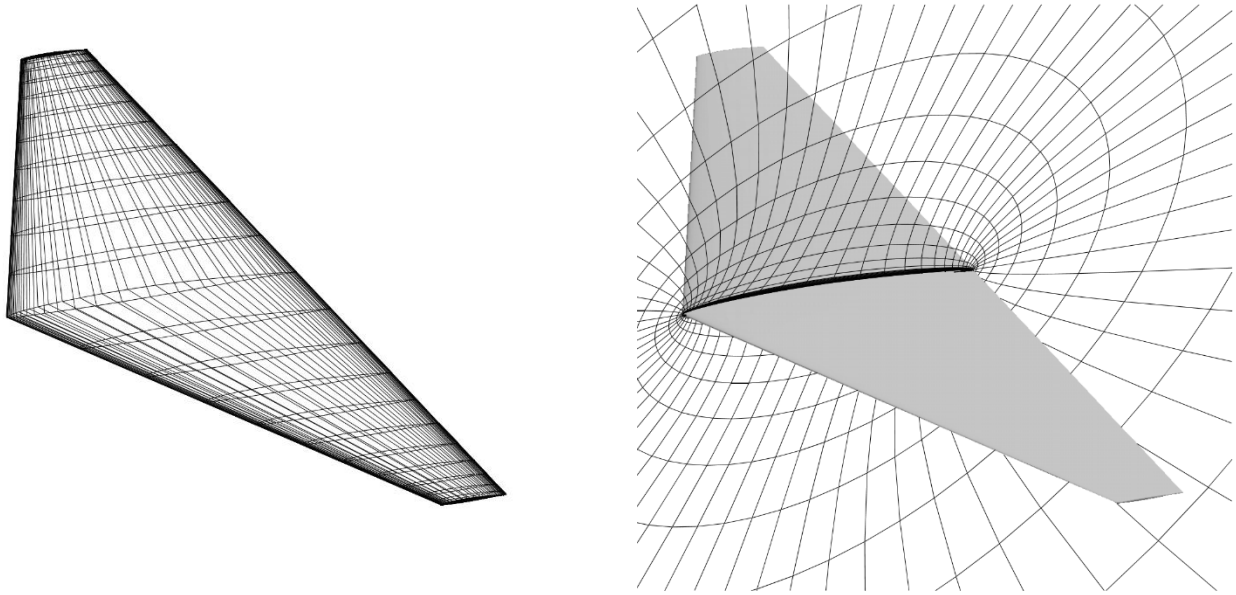

a) b)

Fig. 3 CFD grids of F-16 wing in transonic flow: a) surface grid, b) symmetry plane grid

The exact matched point flutter solution of the wing for Mach=.85 is known as:

Flutter altitude (ft) = -2112.1394

Flutter dynamic pressure (slugs/ft-sec^2) = $1.1545\text{e}+03$

Flutter frequency (Hz) = 8.43

Flutter mode: (1st torsion/1st bending) = $(1.2784 - \text{j}\ 5.3954)$ $(\text{j} \equiv \sqrt{-1})$

Fig. 4 and 5 show the frequency responses of the bending and torsion modes due to the gust at 5,000 ft at Mach=.85. Total of 15 sampling points were placed in $(8, 9)\ Hz$ with six of them in $(8.4, 8.5)\ Hz$ to capture the critical torsion mode accurately. Fig. 6 is Nyquist diagram of $det[\boldsymbol{I}_N - \kappa_f \boldsymbol{\Lambda}_N(\omega)]$ using data obtained at two altitudes, h_0 =5,000 ft and h_1 =4,000 ft. To achieve a higher resolution, the 15 samples were splined up to 200 points in the same range. The two sets of the frequency responses were used to calculate the dynamic eigenmodes and eigenvalues and then κ value was increased to κ_f until the Nyquist plot touched the origin.

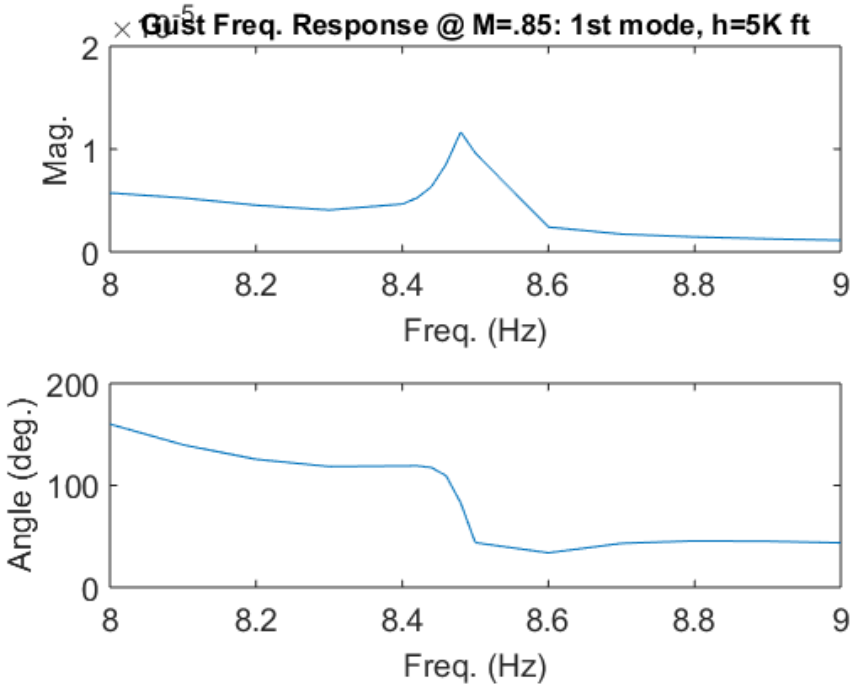

Fig. 4 Frequency response of bending mode due to a uniform gust input @ h=5,000 ft.

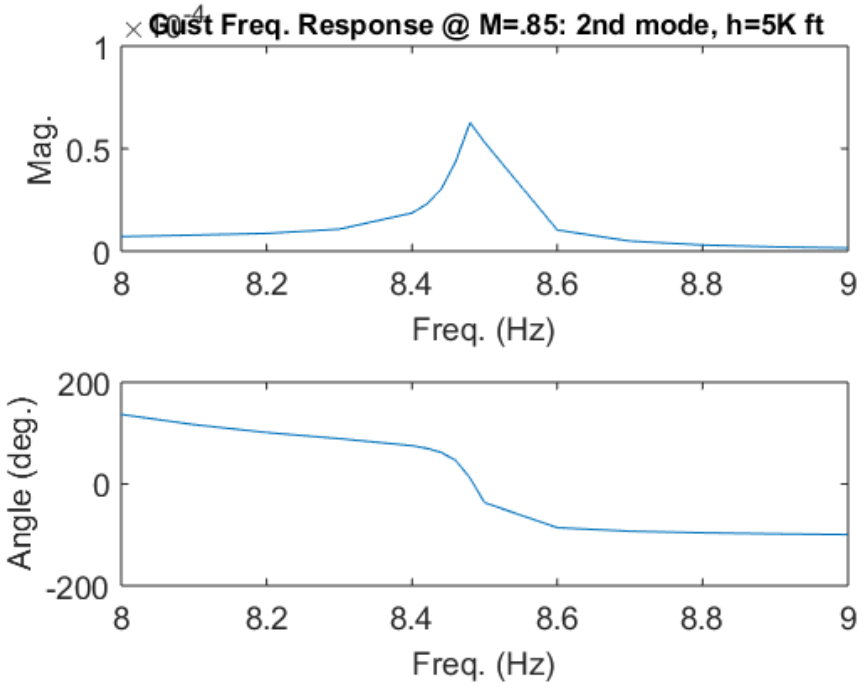

Fig. 5 Frequency response of torsion mode due to a uniform gust input @ h=5,000 ft.

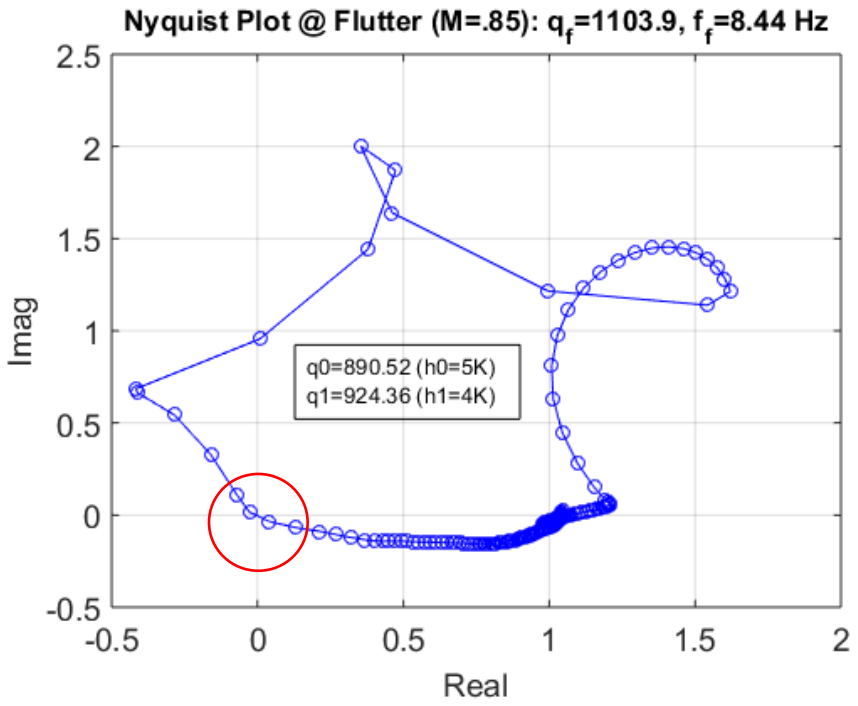

Fig. 6 Nyquist diagram based on the gust freq. responses at h=5,000 ft and 4,000 ft.

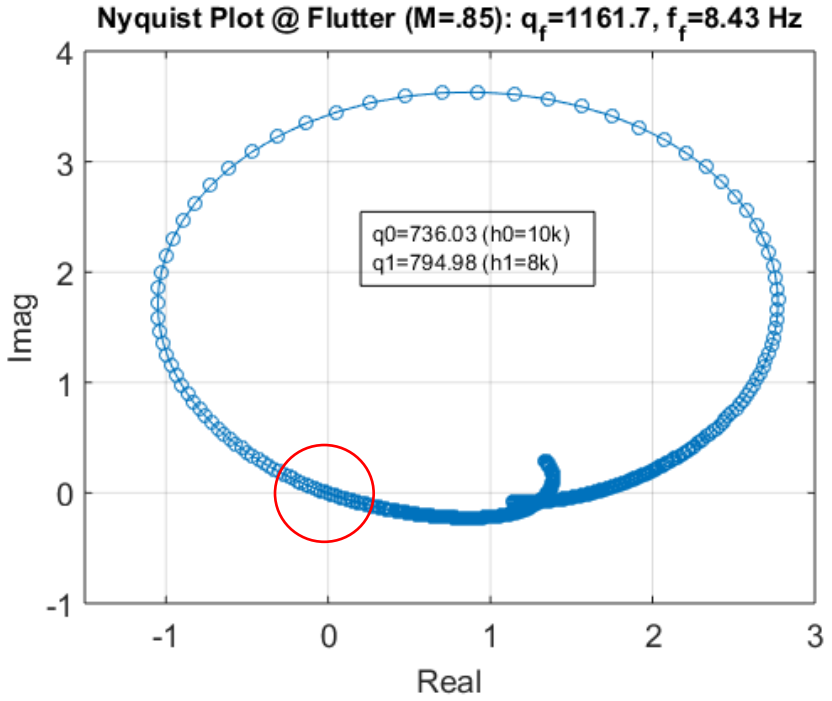

Fig. 7 Nyquist diagram based on the (2×2) AE EQM at h=10,000 ft and 8,000 ft.

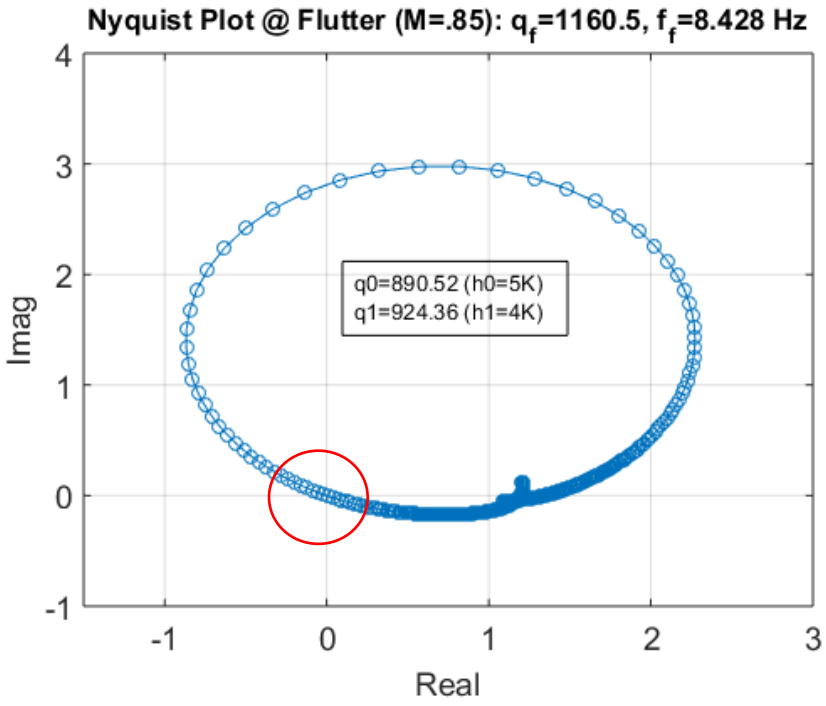

Fig. 8 Nyquist diagram based on the (2×2) AE EQM at h=5,000 ft and 4,000 ft.

The flutter solution found is summarized as:

Flutter dynamic pressure (slugs/ft-sec^2) = $1.1039e + 03$
% Error in q_f = – 4.39%
Flutter frequency (Hz) = 8.44
Flutter mode: (1st torsion/1st bending) = $(1.0392 - j\ 5.4740)$

The error in predicting the critical dynamic pressure is therefore –4.39%, and the identified flutter mode is very close to the exact solution. The next two plots, Figs. 7 and 8 are Nyquist diagrams obtained by executing the DE on the original (2×2) aeroelastic equation of motion, rather than on the gust responses, at two sets of reference points, first at h_0 =10,000, h_1 =8,000 ft, and then h_0 =5,000, h_1 =4,000 ft. For these calculations, the original 15 raw data of the generalized aerodynamic matrices were splined to 1,000 points. The flutter solutions are,

$\underline{h_0 = 10{,}000,\ h_1 = 8000 \text{ ft:}}$

Flutter dynamic pressure (slugs/ft-sec^2) = $1.1617e + 03$
% Error in q_f =.62%
Flutter frequency (Hz) = 8.43
Flutter mode: (1st torsion/1st bending) = $(1.1476 - j\ 5.3425)$

$\underline{h_0 = 5{,}000,\ h_1 = 4{,}000 \text{ ft:}}$

Flutter dynamic pressure (slugs/ft-sec^2) = $1.1605\text{e} + 03$
% Error in q_f=.52%
Flutter frequency (Hz) = 8.43
Flutter mode: (1st torsion/1st bending) = $(1.1476 - \text{j } 5.3425)$

As can be seen, the flutter solutions obtained based on the aeroelastic equation of motion are much closer to the exact solution. This is because, the full transfer function matrix was available without the need for VCI. More importantly, the aerodynamic data, unlike the aeroelastic responses, is smooth and hence using 15 samples yielded excellent fitting. It is, however, difficult to extract the (2×2) generalized aerodynamic matrix from the coupled aeroelastic simulation and for this reason the gust response is preferred for the practical purposes. To improve the flutter prediction based on the gust responses it would be necessary to increase the samples, particularly near the critical resonance frequency. It is seen that regardless of the altitudes at which the data was taken, the method yields essentially the same flutter solutions.

8. CONCLUSIONS

Aircraft flutter has been conducted using the latest flutter prediction method derived based on the Dynamic Eigen Decomposition (DED) technique and coupled CFD-CSD simulations of F-16 wing subject to a uniform vertical gust in a transonic regime. Previously, it was shown that when the perturbed aeroelastic equation of motion is decomposed into the Dynamic Eigenmodes (DE) at a given dynamic pressure, the critical flutter can be predicted by linearly extrapolating the corresponding dynamic eigenvalues in the frequency domain. Furthermore, the flutter mode was identified as one of the DEs and this led to the conclusion that flutter mode is really *an intrinsic property* of the aeroelastic system obtainable at any dynamic pressure. In this study, the basic DED formulation was extended to include possible variations in speed of sound as well as in air density, although it is recognized that the air speed changes only $\pm 7.5\%$ from its mean value in the atmosphere and its influence on flutter is even smaller. It was shown analytically that if the two parameter variations are allowed the flutter mode will be a superposition of two groups of DEs, $\boldsymbol{V}_1(\omega_f)$ for the dynamic pressure variation and $\boldsymbol{V}_2(\omega_f)$ for the air speed variation, implying that the flutter mode can still be regarded as an intrinsic property of the aeroelastic system in the broader sense. For the numerical simulations, aeroelastic responses due to a vertical gust input were calculated at pairs of altitudes. The full aeroelastic equations of motion were also used by extracting the generalized aerodynamic matrices. It was shown that in both types of the simulations, when the calculations are done using the single parameter, dynamic pressure, the predicted flutter solutions are very close to the known exact solution with 4.4% and .6% errors in the critical dynamic pressure values, respectively. However, there might exist certain combinations of aircraft configurations and flight conditions for which the additional variation in air speed could influence flutter significantly and for that it will be necessary to investigate a wide range of flight scenarios using the newly derived formulation. This will be a topic worth exploring in a near future. Lastly, more investigations are recommended using full aircraft simulations and real FFT data.

References:

[1] Kim, T., Surrogate Model Reduction for Linear Dynamic Systems Based on a Frequency Domain Modal Analysis. Computational Mechanics 2015, 56 (4), 709-723.

[2] Kim, T., Parametric model reduction for aeroelastic systems: Invariant aeroelastic modes, Journal of Fluids and Structures 2016, 65: 196-216.

[3] Kim, T., 2018. Higher order modal transformation for reduced-order modeling of linear systems undergoing global parametric variations. International Journal for Numerical Methods in Engineering, 1–22. https://doi.org/10.1002/nme.5905.

[4] Kim, T., Flutter Prediction Methodology Based on Dynamic Eigen Decomposition and Frequency-Domain Stability, submitted to Journal of Fluids and Structures.

[5] Kim, T., Dowell, E.H., 2018. Flutter Prediction Based on Dynamic Eigen Decomposition of Flight Data with Limited Actuators and Sensors. SciTech 2018, January 8-12, Kissimmee, FL, USA.

[6] Kim, T., 2019. Finding characteristically rich nonlinear solution space: a statistical mechanics approach. submitted to International Journal for Numerical Methods in Engineering.

[7] Thomas, J. P., Dowell, E. H., Hall, K. C., and Denegri C. M., "Modeling Limit Cycle Oscillation Behavior of the F-16 Fighter Using a Harmonic Balance Approach," AIAA Paper 2004-1696, 45th AIAA/ASME/ASCE/AHS/ASC Structures, Structural Dynamics and Materials (SDM) Conference, Palm Springs, CA, April 2004.

[8] Thomas, J. P., Dowell, E. H., Hall, K. C., and Denegri, C. M., "Further Investigation of Modeling Limit Cycle Oscillation Behavior of the F-16 Fighter Using a Harmonic Balance Approach," AIAA Paper 2005-1917, 46th AIAA/ASME/ASCE/AHS/ASC Structures, Structural Dynamics and Materials (SDM) Conference, Austin, TX, April 2005.

[9] Thomas, J. P., Dowell, E. H., Hall, K. C., and Denegri, C. M., "An Investigation of the Sensitivity of F-16 Fighter Limit Cycle Oscillations to Uncertainties," AIAA Paper 2006-1847, 47th AIAA/ASME/ASCE/AHS/ASC Structures, Structural Dynamics and Materials (SDM) Conference, Newport, RI, May 2006.

[10] Thomas, J. P., Dowell, E. H., Hall, K. C., and Denegri C. M., "Virtual Aeroelastic Flight Testing for the F-16 Fighter with Stores," AIAA Paper 2007-1640, U.S. Air Force T&E Days, Destin, FL, February, 2007.

[11] Dowell, E. H., Thomas, J. P., Hall, K. C., and Denegri C. M., Jr., "Theoretical Predictions of F-16 Fighter Limit Cycle Oscillations for Flight Flutter Testing," *Journal of Aircraft*, Vol. 46, No. 5, 2009, pp. 1667-1672.